


ORIGINAL ARTICLE

Impaired butyrate absorption in the proximal colon, low serum butyrate and diminished central effects of butyrate on blood pressure in spontaneously hypertensive rats

Tao Yang¹  | Kacy L. Magee¹ | Luis M. Colon-Perez² | Riley Larkin¹ | Yan-Shin Liao¹ | Eliza Balazic¹ | Jonathan R. Cowart¹ | Rebeca Arocha¹ | Ty Redler¹ | Marcelo Febo² | Thomas Vickroy¹ | Christopher J. Martyniuk¹ | Leah R. Reznikov¹ | Jasenka Zubcevic¹

¹Physiological Sciences, College of Veterinary Medicine, University of Florida, Gainesville, Florida

²Department of Psychiatry, College of Medicine, University of Florida, Gainesville, Florida

Correspondence

Jasenka Zubcevic, Physiological Sciences, College of Veterinary Medicine, University of Florida, Gainesville, FL.
Email: jaskaz@ufl.edu

Present address

Tao Yang, Department of Physiology and Functional Genomics, College of Medicine, University of Florida, Gainesville, Florida.

Funding information

American Heart Association, Grant/Award Number: 14SDG18300010; UF CVM Start Up Funds

Abstract

Aim: Butyrate is a major gut microbiota-derived metabolite. Reduced butyrate-producing bacteria has been reported in the spontaneously hypertensive rat (SHR), a model of hypertension characterized by dysfunctional autonomic nervous system and gut dysbiosis. Here, we demonstrate a potential mechanism for butyrate in blood pressure regulation.

Methods: High-performance liquid chromatography and liquid chromatography-mass spectrometry were performed to measure butyrate levels in feces and serum. Ussing chamber determined butyrate transport in colon *ex vivo*. Real-time PCR and immunohistochemistry evaluated expression of butyrate transporter, Slc5a8, in the colon. Mean arterial blood pressure was measured in catheterized anesthetized rats before and after a single butyrate intracerebroventricular injection. Activity of cardioregulatory brain regions was determined by functional magnetic resonance imaging to derive neural effects of butyrate.

Results: In the SHR, we demonstrated elevated butyrate levels in cecal content, but diminished butyrate levels in circulation, possibly due to reduced expression of Slc5a8 transporter in the colon. In addition, we observed lower expression levels of butyrate-sensing receptors in the hypothalamus of SHR, likely leading to the reduced effects of centrally administered butyrate on blood pressure in the SHR. Functional magnetic resonance imaging revealed reduced activation of cardioregulatory brain regions following central administration of butyrate in the SHR compared to control.

Conclusion: We demonstrated a reduced availability of serum butyrate in the SHR, possibly due to diminished colonic absorption. Reduced expression of butyrate-sensing receptors in the SHR hypothalamus may explain the reduced central responsiveness to butyrate, indicating microbial butyrate may play a role in blood pressure regulation.

KEYWORDS

absorption, blood pressure, butyrate, gut microbiota, neuronal activity

1 | INTRODUCTION

Gut dysbiosis is associated with rodent and human hypertension (HTN)^{1–3}; however, the precise mechanisms of host-microbiota interaction in HTN are yet to be elucidated. Butyrate, a major metabolite produced by gut bacterial fermentation, reportedly exerts multiple beneficial effects on the host, including enhancement of intestinal barrier,^{4,5} regulation of immune activation,^{6,7} and inhibition of carcinogenesis,^{8,9} among others. The spontaneously hypertensive rat (SHR) with fully developed HTN shows decreased levels of butyrate-producing bacteria in the gut,³ suggesting a role for this short chain fatty acid (SCFA) in regulation of blood pressure (BP). Furthermore, data from the SPRING study (the Study of Probiotics in Gestational Diabetes) shows a negative correlation between systolic BP (SBP) and abundance of butyrate bacterial producers in the gut microbiota of overweight and obese pregnant women.¹⁰ Lastly, Kim et al recently demonstrated that supplementation of butyrate significantly lowered BP in angiotensin II (Ang II)-infused mouse model of HTN¹¹ while reduced circulating butyrate has recently been reported in hypertensive patients.¹¹ All these combined indicate a significant role for butyrate in BP control.

Consistent with this, Pluznick et al¹² have shown that intravenous application of propionate, another major SCFA, transiently reduces BP in a dose dependent manner. This BP-lowering effect was mediated via GPR41, a vascular SCFA receptor. In addition to the vasculature,^{12,13} the SCFA-sensing receptors OLF78 and GPR43, as well as GPR41, are reportedly present on the sympathetic ganglia^{14,15} and spleen.^{16,17} Thus, the presence of SCFA-sensing receptors in diverse tissues implies that SCFAs may exert their BP-regulating effects via modulation of vascular responsiveness,^{12,13} sympathetic activity¹⁴ and immune responses.^{16,17} Furthermore, butyrate is reportedly able to cross the blood brain barrier (BBB) via specific butyrate transporters,^{18–20} suggesting its potential for direct central effects.²¹ Previous findings determined expression levels of SCFA-sensing receptors in the whole brain lysates,¹⁴ but no studies to date have specifically examined the expression of these receptors in cardioregulatory brain regions such as the paraventricular nucleus (PVN) of the hypothalamus. Indeed, butyrate is thought to actively participate in regulation of the nervous system homeostasis, as demonstrated both in vitro and in vivo. Huuskonen et al²² utilized multiple cell models (ie, primary microglia, hippocampal slice cultures and co-cultures of microglial cells, astrocytes and cerebella granule neurons) to demonstrate that butyrate is anti-inflammatory in the face of immune challenges. Others have also suggested a beneficial role for butyrate in the enhancement of BBB integrity.²³ Finally, two research groups^{24,25} have reported that butyrate can also promote

production of serotonin, another major BP regulator that acts both in the periphery and centrally.²⁶ Collectively, these findings suggest a potential for a significant role for butyrate in central control of BP.

Our previous work showed a decrease in butyrate-producing bacteria in the SHR,⁹ a model of neurogenic HTN characterized by sustained age-dependent elevation in sympathetic activity and BP^{27–29} and marked by elevated peripheral immune responses and neuroinflammation.^{30,31} Moreover, in vitro application of butyrate produced anti-inflammatory responses and lowered expression of Ang II receptor in the SHR astrocytes.³² From this, we hypothesized that circulating butyrate contributes to BP regulation by in part acting on central cardioregulatory mechanisms that are perturbed in the SHR. Our novel data show that decreased circulating butyrate may be a consequence of reduced butyrate transport from the gut into circulation, while low levels of SCFA receptors in the PVN region may account for the diminished cardioregulatory neuronal responses to central butyrate administration in the SHR. We propose that the observed changes in the gut butyrate transporter expression but not in the expression of the brain SCFA receptors may partially be due to epigenetic modification, as we observed increased histone acetylation in the gut but not the hypothalamic brain region of the SHR.

2 | RESULTS

2.1 | Transport of butyrate across the proximal colon is impaired in the SHR

We previously showed a reduction in the butyrate-producing bacteria in the hypertensive SHR compared to WKY rats.³ However, no analysis of the levels of bacterial end products in the gut and circulation of SHR has been performed to date. Therefore, we evaluated the levels of three major SCFAs in feces collected from the cecum of juvenile (4 weeks old) and adult (14 weeks old) WKY rats and SHR using high performance liquid chromatography (HPLC; Figures 1A and S1A, B). Circulating butyrate levels were also determined in both strains and ages by liquid chromatography–mass spectrometry (LC-MS; Figure 1B). In the juvenile WKY and SHR, no difference was observed in the cecal butyrate levels (Figure 1A). However, cecal butyrate was higher in the adult SHR compared to age-matched WKY rats (WKY $18.56 \pm 1.54 \mu\text{mol/g}$ vs SHR $27.93 \pm 1.732 \mu\text{mol/g}$, $N = 10/11$, $P = 0.004$; Figure 1A). We also demonstrated a consistent reduction of serum butyrate in the SHR, compared to WKY in both juvenile (WKY $1.71 \pm 0.37 \mu\text{mol/L}$ vs SHR $0.47 \pm 0.091 \mu\text{mol/L}$, $N = 4/3$, $P = 0.0005$) and adult rats (WKY $1.23 \pm 0.14 \mu\text{mol/L}$ vs SHR $0.23 \pm 0.033 \mu\text{mol/L}$, $N = 4$, $P = 0.0005$; Figure 1B).

In addition, we compared the SCFAs' levels in the fecal contents collected from proximal and distal colon (Figures 2A and S1C,D). Consistent with previous publications,^{33,34} butyrate appeared to be primarily absorbed/utilized in the proximal colon (Figure 2A,B). However, lower levels of butyrate in the serum of adult SHR compared to WKY (Figure 1B) suggested a compromised transport of butyrate in the SHR.

To investigate butyrate transport, absorption and/or utilization in the proximal colon of SHR, we utilized the Ussing chamber.³⁵ Specifically, we excised proximal segments of the colon and mounted them in the Ussing chamber as described in the methods. The experiment was initiated with the addition of butyrate (40 mmol/L) to the apical (luminal) side of the proximal colon tissue of adult WKYs and SHRs. One hour later, we observed approx. 200-fold lower concentrations of butyrate on the basolateral (serosal)

side of the proximal colon in the SHR compared to the WKY (WKY 0.24 ± 0.088 mmol vs SHR 0.0099 ± 0.001 mmol, $N = 4$ per group, $P = 0.026$; Figure 2C). These data suggest that there is dysfunctional transport of butyrate across the proximal colon into the serosal side. Further evidence to support this claim was found by examining the amount of butyrate utilized by the tissues. To do this, we calculated the difference in total butyrate detected on the apical and basolateral sides of the chamber after 1-hour incubation and compared the total butyrate administered to the chamber at the beginning of the experiment. We found no differences in the levels of utilized butyrate by the proximal colon of adult WKY rat and SHR using this method (Figure 2C).

Lastly, we examined the responses of short circuit current (Isc) to butyrate, as previous reports indicated that butyrate-HCO₃⁻ exchange is one of the main apical butyrate

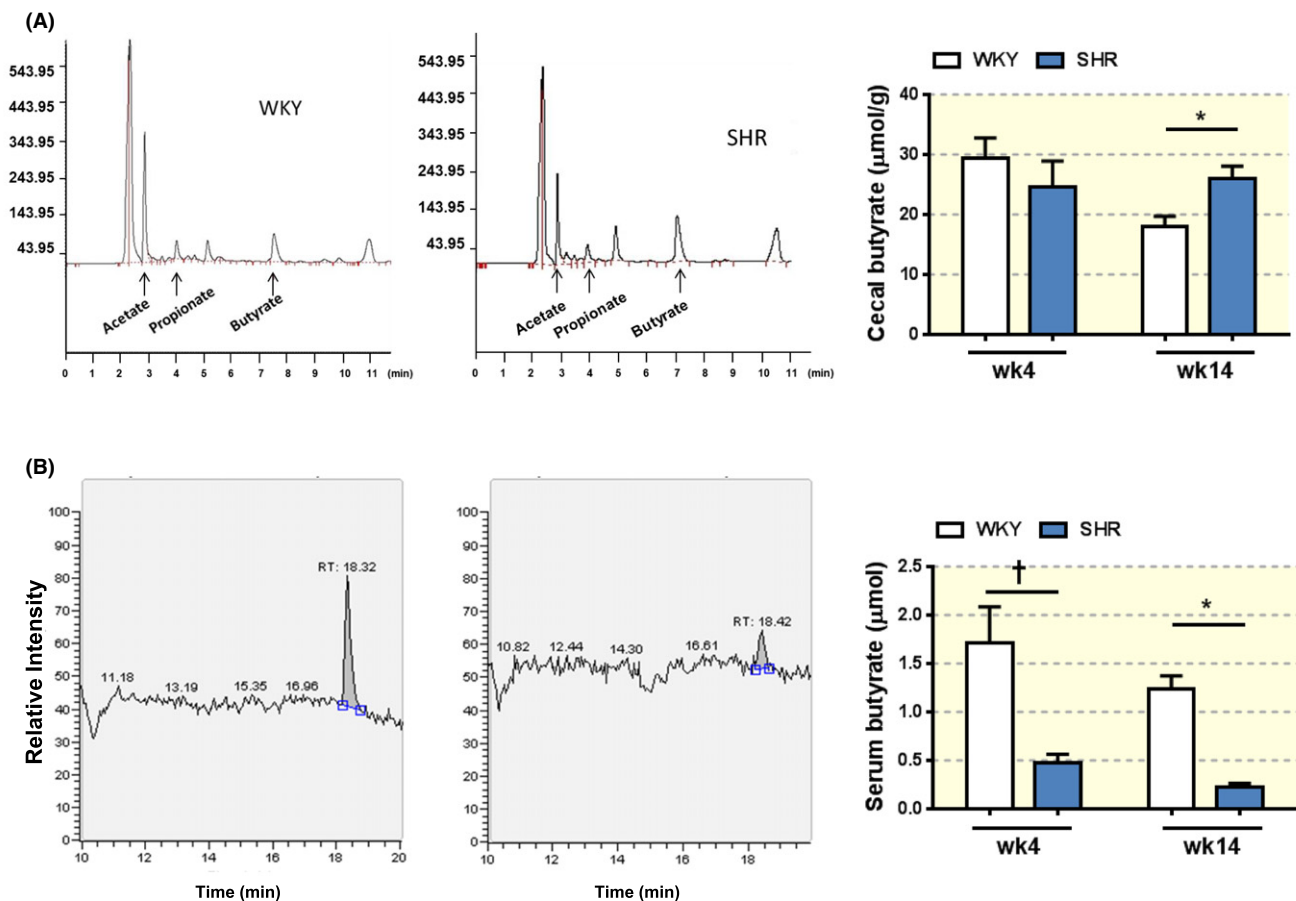


FIGURE 1 Levels of butyrate in the cecum and serum in juvenile and adult WKY and SHR. A, Representative peaks for three SCFAs, acetate, propionate and butyrate in the cecal contents from adult (14 weeks old, wk14) WKY (A, left panel) and SHR (A, middle panel) as measured by HPLC. Absolute cecal levels of butyrate were determined in adult and juvenile (4 weeks old, wk4) WKY and SHR (A, right panel). Two-way ANOVA was performed with Sidak's multiple comparison test. * $P < 0.05$, † $P < 0.01$. B, Representative LC-MS figures show typical peaks for butyrate in serum from adult WKY (B, left panel) and SHR (B, middle panel). Absolute butyrate levels in the serum of juvenile and adult WKY and SHR were determined by LC-MS (B, right panel). Two-way ANOVA was performed with Sidak's multiple comparison test. * $P < 0.05$, † $P < 0.01$

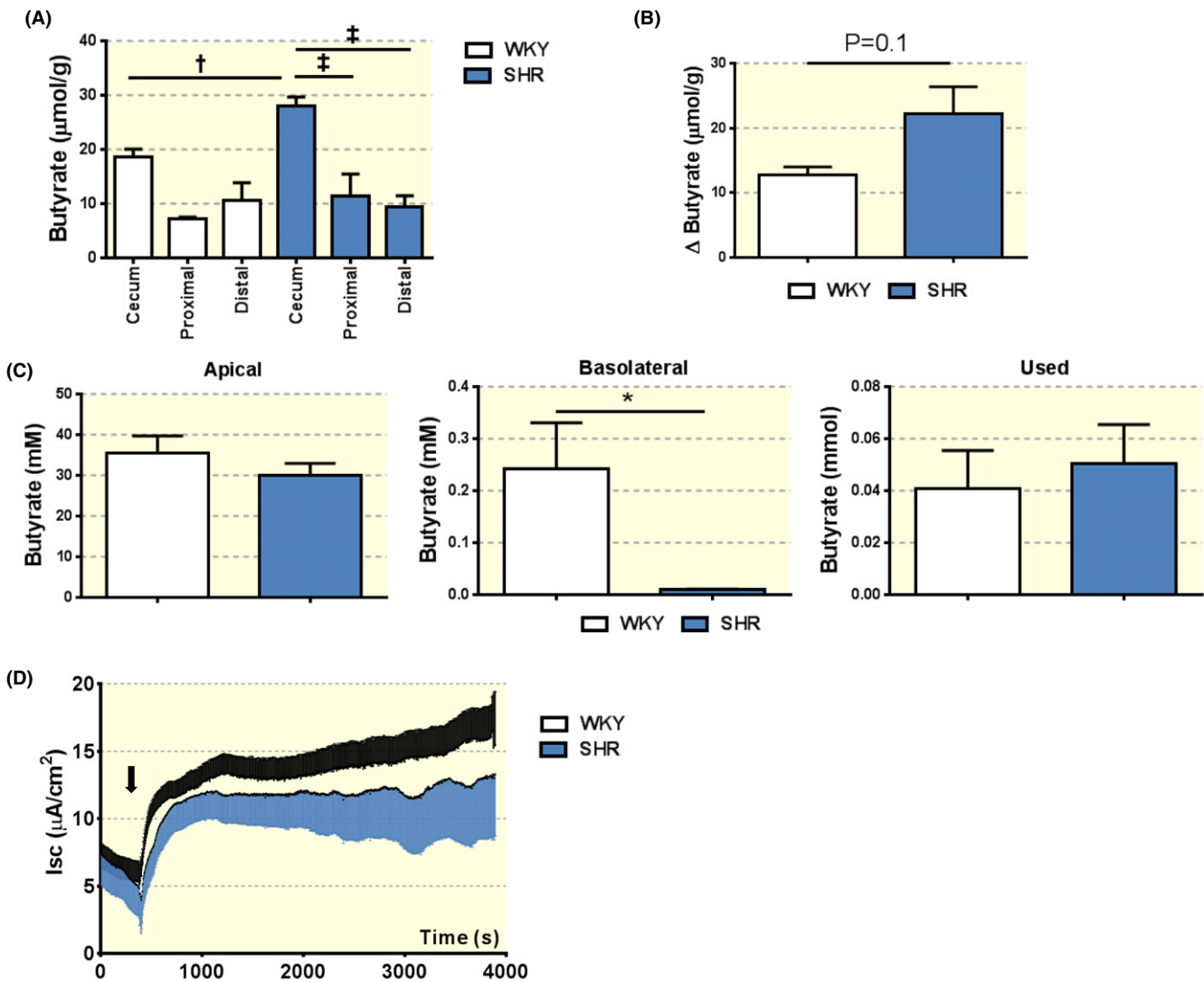


FIGURE 2 Impaired butyrate transport across the proximal colon epithelium in the SHR. A, Butyrate levels in the cecum, proximal and distal colon of adult WKY and SHR. Fecal samples were collected at indicated segments of the intestine, and subjected to HPLC for measurement of butyrate levels. One-way ANOVA was performed with Sidak's multiple comparison test. $*P < 0.05$, $^\dagger P < 0.01$, $^\ddagger P < 0.001$. B, Decrease in butyrate levels in proximal colon relative to cecum of adult WKY and SHR. Unpaired t -test $P = 0.1$. C, Butyrate absorption in the proximal colon of adult WKY and SHR. Proximal colon was isolated from adult WKY and SHR and mounted in the Ussing chamber. Krebs buffer containing 40 mmol/L butyrate was applied on the apical side of the proximal colon. One hour following the incubation, butyrate levels in both apical and basolateral solutions were determined by LC-MS. "Used" butyrate represents the difference between total butyrate initially applied to the chamber and the butyrate levels in the apical and basolateral solutions. $*P < 0.05$ in unpaired t -test. D, Short circuit current measurements (Isc) show no difference in proximal colon ionic transport between WKY and SHR at baseline and upon addition of butyrate. The black arrow indicates addition of butyrate to the apical side of proximal colon

uptake mechanisms.³⁶ We found no significant differences in Isc in adult SHR compared to WKY following butyrate (Figure 2D). Quantification revealed no differences in Isc between WKY and SHR at baseline, during the first 10 minute post butyrate application, or during the last 10 minute post-application (Figure S2). Thus, these findings suggested that the low levels of butyrate in the serum of adult SHR may be partially due to the impaired butyrate transport in the proximal colon, and not due to differences

in utilization of butyrate by the proximal colon cells in the SHR.

2.2 | Relative expression levels of SCFA transporters in the proximal colon of WKY and SHR

We tested relative expression levels of three monocarboxylate transporters reportedly involved in butyrate and

other SCFA transport into and across the gut epithelial cells.^{21,37} Relative expression levels of *Slc5a8* were significantly decreased in the proximal colon of SHR compared to WKY rats (*Slc5a8*, WKY 0.028 ± 0.0063 vs SHR 0.065 ± 0.012 , $N = 4$, $P = 0.0325$; Figure 3A). In line with this, immunohistochemical examination of proximal colon revealed lower protein levels of *Slc5a8* in the luminal epithelial cells of SHR compared to WKY (WKY 270.3 ± 2.59 vs SHR 188.1 ± 8.89 , $N = 3/4$, $P = 0.0006$; Figure 3B). This result suggested that decreased SCFA transporters might account for the decreased amount of serum butyrate observed in vivo and decreased transport of butyrate across colon epithelium ex vivo.

2.3 | Acetylation of histone H3 in the proximal colon and hypothalamus

Butyrate is a potent histone deacetylase inhibitor³⁸; thus we investigated total acetylation levels in the proximal colon and hypothalamus of SHR and WKY by Western blot. Following normalizing for total protein, we observed higher levels of acetylated histone H3 in the proximal colon in

SHR, compared to that in WKY (WKY $1.424 \times 10^7 \pm 7.983 \times 10^6$ vs SHR $4.567 \times 10^7 \pm 7.019 \times 10^6$, $N = 6$, $P = 0.0146$, Figure 4A,B). We observed no difference in total H3 levels in the proximal colon of WKY and SHR (Figure 4A,B). No differences were observed in either acetylated or total histone H3 in the hypothalamus of WKY and SHR (Figure 4C,D).

2.4 | Reduced expression of SCFA-sensing receptors in the SHR hypothalamus

We tested the relative expression levels of SCFA-sensing receptors in the hypothalamic PVN to evaluate the potential for direct actions of butyrate on this cardioregulatory brain region. We observed reduced relative expression levels of *Olfir59* (WKY $0.00058 \pm 3.4e-005$ vs SHR $0.00039 \pm 4.0e-005$, $N = 4/3$, $P = 0.0134$) and *Ffar3* (WKY $0.0002 \pm 2.7e-005$ vs SHR $6.9e-005 \pm 1.9e-005$, $N = 4/3$, $P = 0.0152$) in the hypothalamus of SHR compared with WKY (Figure 5A). Thus, the machinery to sense butyrate appeared to be partially compromised in the SHR hypothalamus.

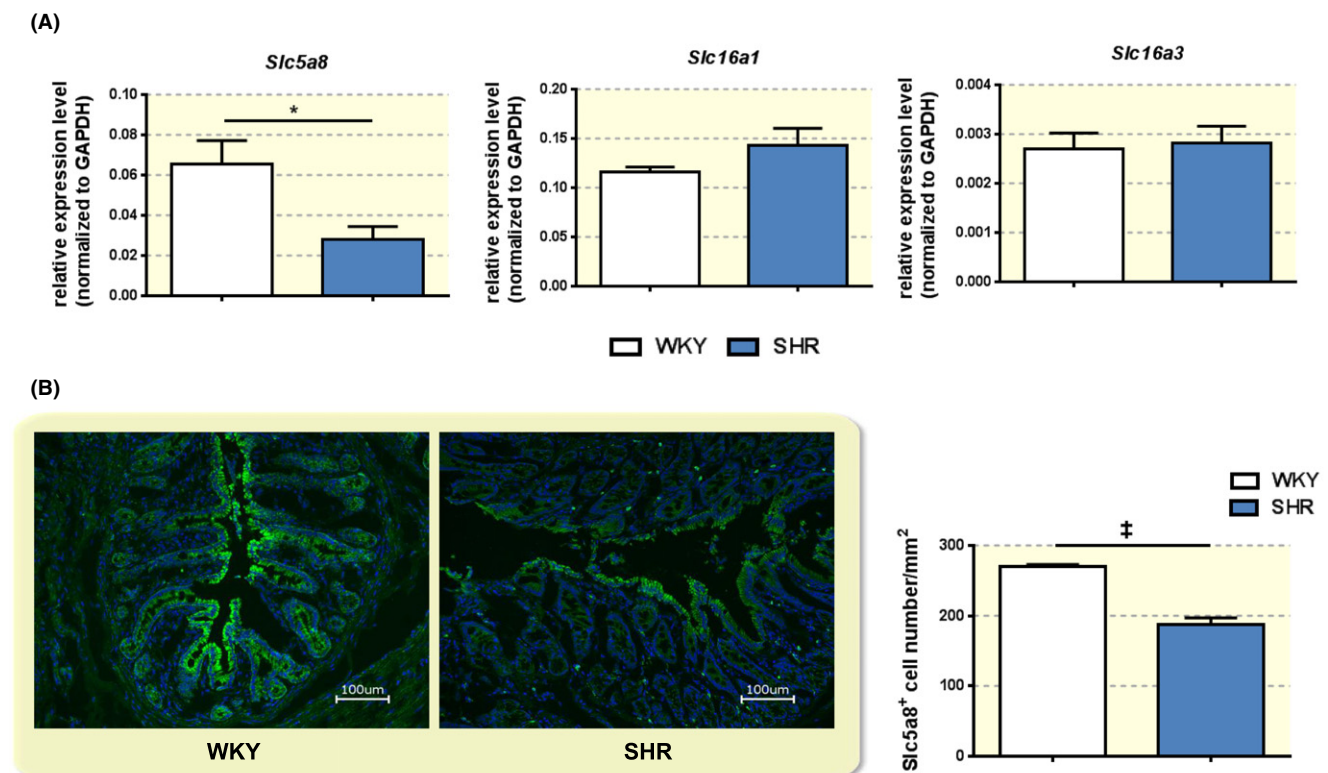


FIGURE 3 Decreased butyrate transporter *Slc5a8* in the proximal colon of SHR. A, Relative expression levels of specific SCFA transporters *Slc5a8*, *Slc16a1* and *Slc16a3* were determined by quantitative real time PCR in the proximal colon of adult WKY and SHR. * $P < 0.05$ by unpaired t -test. B, Immunohistochemistry and quantification of *Slc5a8* in the proximal colon of adult WKY and SHR. Note the expression of *Slc5a8* is mainly within the epithelial cells on the apical side of the colon. ‡ $P < 0.001$ by unpaired t -test

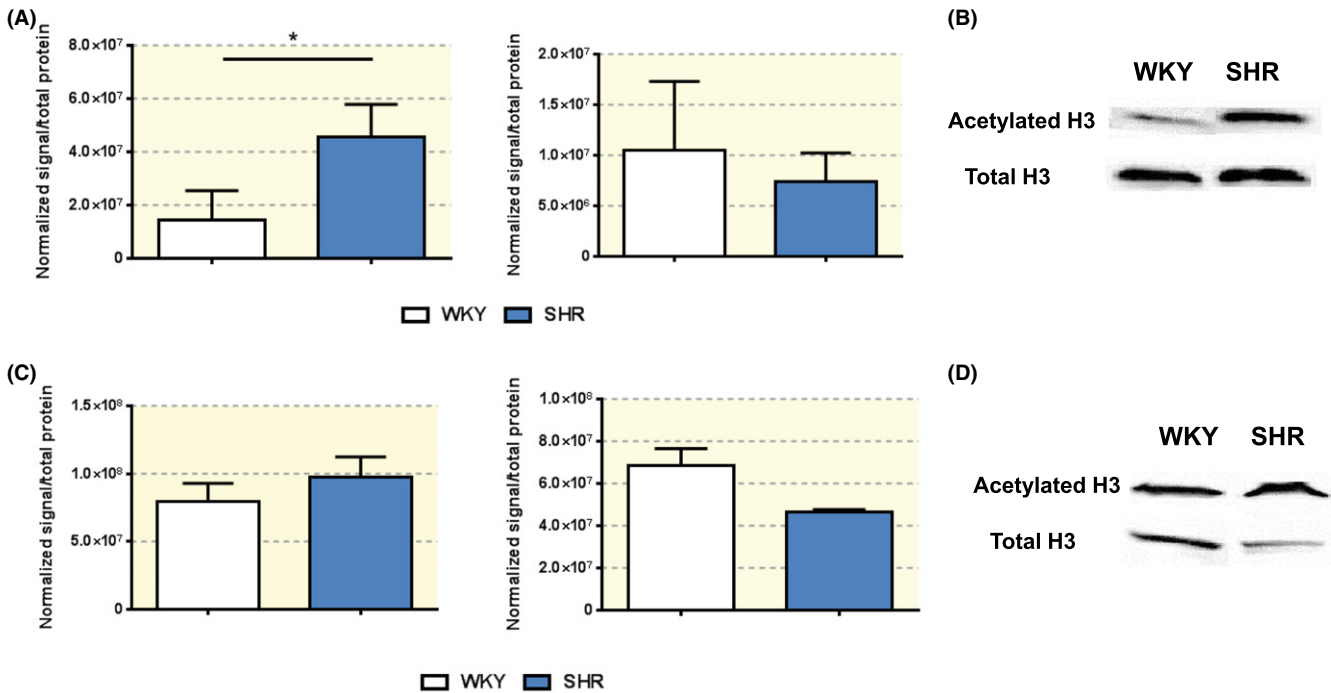


FIGURE 4 Acetylation of histone H3 in the proximal colon and hypothalamus of WKY and SHR. A, Western blot in the proximal colon of adult WKY and SHR shows total acetylated histone 3 (H3) protein levels (far left panel) and total H3 protein levels (middle panel), with representative blots, normalized for total protein loaded onto gel, showed in B. $*P < 0.05$ by unpaired *t*-test, Welch correction. C, Western blot in the hypothalamus of adult WKY and SHR shows total acetylated histone 3 (H3) protein levels (far left panel) and total H3 protein levels (middle panel), with representative blots, normalized for total protein loaded onto gel, showed in D, Unpaired *t*-test, Welch correction

2.5 | ICV injection of butyrate decreases BP and modifies neuronal activity in cardioregulatory brain regions of anesthetized rats

Considering the reduced levels of hypothalamic SCFA-sensing receptors in the SHR, we next tested the effect of central administration of butyrate in regulation of BP in adult anesthetized WKY and SHR. ICV injections of butyrate resulted in a significantly greater decrease in BP in the WKY compared with SHR, at 400 seconds following the injection (WKY -7.56 ± 2.13 mm Hg vs SHR -2.59 ± 0.49 mm Hg, $N = 5/6$, $P = 0.0235$), and 1000 seconds following the injection (WKY -20.027 ± 1.05 mm Hg vs SHR -13.07 ± 0.78 mm Hg, $N = 5$, $P = 0.05$; Figure 5B). The timing of butyrate effects on BP may be attributed to timing of butyrate diffusion within the brain ventricular system, rather than its effects on cell signaling pathways or central immune system.

To identify specific brain regions that respond to central butyrate, we performed functional magnetic resonance imaging (fMRI) in anesthetized WKY and SHR. In line with our BP and SCFA receptors data, several cardioregulatory brain regions, including the hypothalamus and brainstem regions, showed lower neuronal activation in the SHR

compared to WKY following ICV butyrate administration (Figures 5C,D, and S3).

3 | DISCUSSION

Given the significant contraction of butyrate-producing bacteria in established HTN,³ in addition to reported systemic effects of propionate on BP,¹² we aimed to determine absolute butyrate levels in the intestine and circulation, and investigate central effects of butyrate on BP in WKY and SHR. The most significant observations of this study include: (a) poor transport of butyrate across proximal colon and reduced expression of a specific SCFA transporter, Slc5a8 in the proximal colon may lead to lower butyrate levels in the serum and consequently trapping of butyrate in the proximal colon of SHR; and (b) reduced expression of SCFA-sensing receptors in the PVN of hypothalamus may be the cause of reduced central effects of exogenously applied butyrate on BP and diminished neuronal activation by butyrate in anesthetized SHR.

There is a growing appreciation for the role of gut microbiota in modulation of both brain function and BP.^{39–41} Reciprocally, pathological alterations in the brain such as those observed in autism spectrum disorder and mood disorders among others have been linked to intestinal

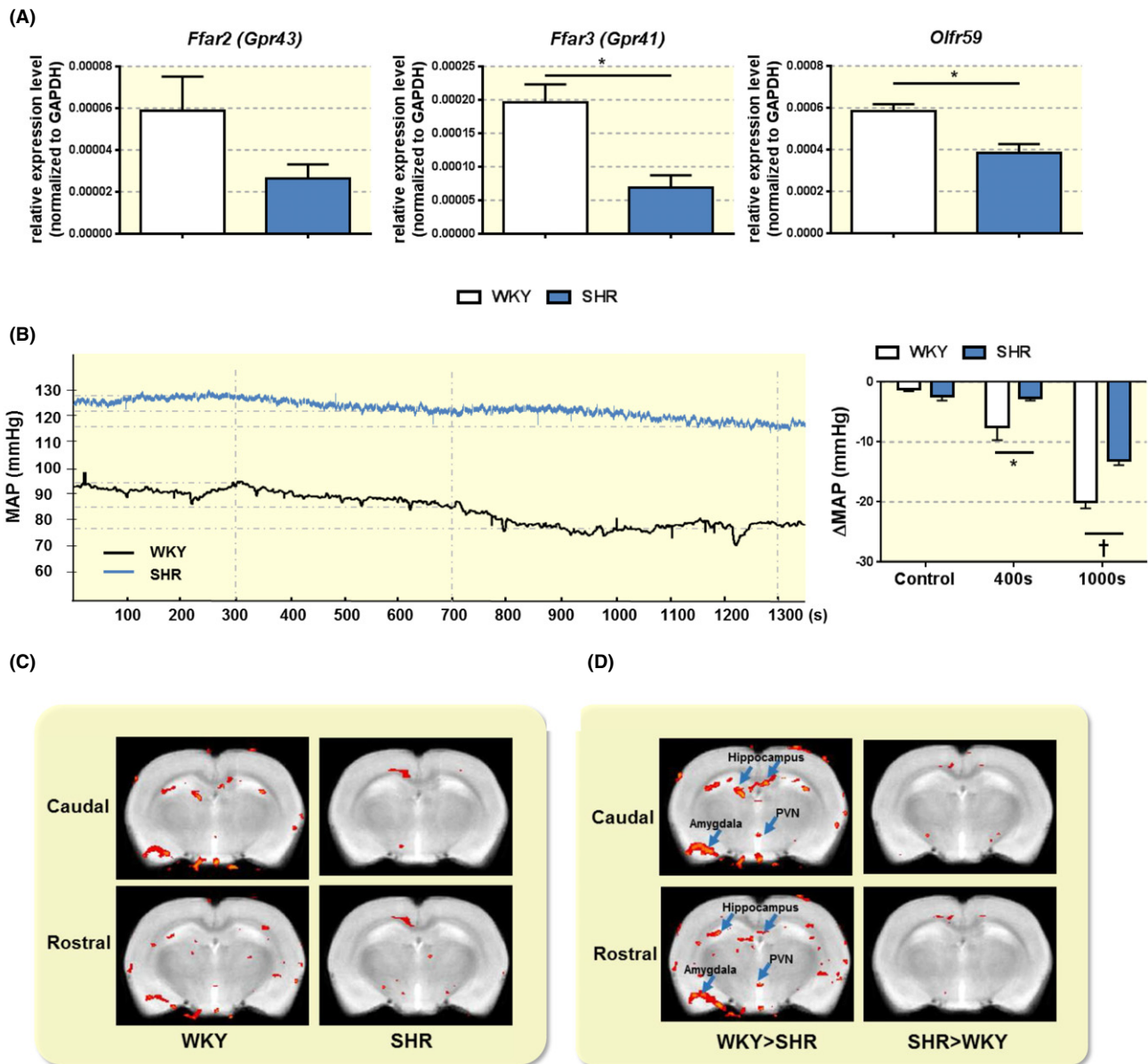


FIGURE 5 Reduced relative expression levels of SCFA-sensing receptors in hypothalamus and reduced effect of ICV butyrate on mean arterial pressure (MAP) and activation of brain regions in the SHR. A, Total RNA from hypothalamus of adult WKY and SHR was isolated and subjected to real time PCR analysis of relative expression of SCFA receptors *Ffar2*, *Ffar3* and *Olfr59*. * $P < 0.05$ by unpaired *t*-test. B, Representative tracings of MAP in anesthetized adult WKY and SHR. WKY and SHR rats were acutely microinjected with 1 μ L of 1 mmol/L butyrate ICV. MAP was monitored in real time via a femoral artery catheter connected to Spike2. Dotted vertical line represents time of MAP analysis following butyrate injection. In the far right panel, ICV injection of butyrate produced a larger decrease in MAP in the WKY compared to the SHR. The bar graph indicates average reduction in MAP at 400 and 1000 s following butyrate injection. * $P < 0.05$ and † $P < 0.001$ by unpaired *t*-test. C, Effect of equivalent ICV injection of butyrate on neuronal activation in specific brain regions of interest (ROIs) in anesthetized adult WKY and SHR as measured by functional magnetic resonance imaging (fMRI). Butyrate injection produced pronounced neuronal activation in several brain regions of the WKY, including the hippocampus, amygdala and hypothalamic paraventricular (PVN). Average volume of activation of specific ROIs in WKY and SHR is presented in the left panel and the right panel respectively, depicting neuronal activation immediately following ICV butyrate injection. D, Relative comparison of WKY and SHR butyrate-dependent fMRI responses. Images on the left show the ROIs with stronger butyrate-dependent signal in the WKY (WKY > SHR), while images on the right show the ROIs with stronger butyrate-dependent signal in the SHR (SHR > WKY) immediately following a single ICV butyrate injection. Caudal and rostral panels represent -1.7 mm and -2.3 mm from Bregma as per Paxinos and Watson Rat Brain Atlas

disorders.^{42,43} Thus, the bidirectional gut-brain axis may be important in the onset and progression of multiple diseases. Here, we show further evidence of deregulation of this axis

in HTN. As previously shown, the adult SHR presents with less butyrate-producing bacteria,³ suggesting lower levels of butyrate in the gut of SHR. However, our current

findings paint a more complex picture and hint to additional deregulated mechanisms of transport of butyrate in the colon. Here, we show that significant absorption of butyrate occurs in the proximal colon in both WKY and SHR, consistent with previous findings.^{33,34} However, reduced levels of butyrate in the blood sera, despite higher levels of butyrate in the colon of SHR compared to WKY, in combination with *ex vivo* reduced ability of butyrate to cross to the serosal side of the proximal colon in the SHR, suggest a dysfunctional mechanism of its absorption into the circulation. It is noteworthy that the capability of liver to metabolize butyrate may also differ between WKY and SHR, but the majority of butyrate is reportedly consumed by the intestinal epithelium.^{44,45} In line with this, impaired transport of butyrate from apical to serosal side in the proximal colon of SHR may be related to decreased levels of Slc5a8, a SCFA transporter present on the colonic epithelium and reportedly responsible for transport of SCFAs across the gut epithelium into the circulation.²¹ This reduction in SCFA transporter is in addition to the previously reported pathophysiological changes in the SHR gut.⁴⁶ Hence, butyrate appears to be trapped inside the SHR colon unable to cross the epithelium. Our data point to novel mechanisms that may contribute to dysfunctional gut-brain axis in HTN.

The serum levels of butyrate were also lower in the 4 week old juvenile SHR. Considering its reported beneficial effects on overall homeostasis,^{38,47} we speculate that reduced circulating levels of butyrate may be a part of pathogenesis of HTN in this rat strain. SHR is characterized by chronic activation of sympathetic nervous system that contributes to elevated BP.^{29,48} Our gene expression data for the first time confirm the presence of SCFA-sensing receptors in the PVN of hypothalamus, a major brain region involved in regulation of the sympathetic output. As butyrate is able to cross the BBB,^{18–20} circulating butyrate may thus have direct effects on the brain regions regulating BP. Indeed, our data showed that ICV injection of butyrate significantly lowered BP in both the WKY and SHR, albeit at a significantly reduced levels in the SHR. We also observed downregulated butyrate-sensing receptors in the hypothalamus of the SHR, suggesting that lower availability of butyrate in circulation coupled with its lowered action on the brain cardioregulatory region (eg, hypothalamus) may contribute to the increased blood pressure in the SHR. Further studies are needed to directly prove this hypothesis.

Previously, several groups have reported the presence of SCFA-sensing receptors (ie, GPR41, OLF59) in multiple organs and neural tissues, including the superior cervical ganglion, sympathetic ganglia of the thoracic and lumbar sympathetic trunk, vagal ganglia, adrenal medulla, kidney and spleen.^{14,15} Moreover, the effects of SCFA on

modulation of sympathetic activity and BP have also previously been suggested. Kimura et al¹⁴ observed reduced circulatory noradrenaline levels in the Gpr41^{-/-} mice. Additionally, IP administration of propionate caused a significant increase in heart rate in the wild type, but not the Gpr41^{-/-} mice. In a separate study, Pluznick et al¹² showed that IV application of propionate caused a dose-dependent drop in BP in the wild type mice. However, this effect was blunted in the Gpr41^{-/-} mice. Thus, SCFAs including butyrate may have a direct effect on the nervous system involved in control of BP. This introduces an interesting discussion on several possible modes of action and target mechanisms of SCFAs that needs to be further explored. One such long-term mechanism of action may involve epigenetic modification of gene expression. Butyrate is a potent histone deacetylase (HDAC) inhibitor³⁸; indeed, SCFA transporters like those investigated in the current study can be directly regulated by SCFAs^{49,50}; thus, the possibility that butyrate can directly modulate the expression of its own transporter in the proximal colon should be further explored for therapeutic purposes. We did not observe H3 changes in the brain of SHR, however, one rat study, did show evidence of epigenetic regulation in the brain by butyrate in cocaine-administered rats.⁵¹ However, the epigenetic effects described in the mentioned study occurred at 24 hours following administration of both cocaine and butyrate, whereas the present study shows for the first time an immediate neuronal response to central butyrate. This supports the existence of functional binding sites for butyrate that modulate neuronal activity, particularly in central cardioregulatory regions.

A potential shortcoming of using fMRI, compared with manganese enhanced MRI, is its relative low resolution, which prevents from accurately locating activation in smaller subnuclei. However, the responses near the PVN, amygdala and hippocampus were robust and measurable. In addition to the BP-regulating hypothalamic PVN, our fMRI data also showed that ICV butyrate caused changes in neuronal activity in other cardioregulatory, emotion- and cognition-related regions,^{52–54} and most notably amygdala, hippocampus and brainstem regions, again to a lower extent in the SHR. This suggests that butyrate may also potentially impact behavior, emotion and cognition³⁸ in addition to BP. Studies related to butyrate-associated behavioral changes need to be further explored due to the largely contentious data present in the literature. For example, Gagliano et al⁵² showed that IP administration with high dose (1200 mg/kg), but not low dose (200 mg/kg) of butyrate induced stress-like responses in male rats, characterized by elevation of adrenocorticotrophin hormone (ACTH) and corticosterone levels in plasma, and increased c-fos expression in the amygdala and PVN. Valvassori et al⁵³ demonstrated that the IP injection of butyrate

(500 mg/kg) attenuated depressive-like behavior in Wistar rats. Consistent with this, Han et al⁵⁴ observed similar mitigation of depressive-like behavior by IP injection of butyrate (600 mg/kg) in the ICR mice with chronic restraint stress. Unsurprisingly, changes in histone acetylation levels were also documented in studies investigating memory retention and contextual fear learning that are associated with amygdala and hippocampus brain regions. Therefore, it is possible that different levels of availability of butyrate and in specific tissues can differentially affect gene expression and thus physiological responses.

Collectively, our data suggest that reduced circulating butyrate levels in the SHR, possibly as a result of dysfunctional butyrate transport in the SHR intestine, may contribute to the hypertensive phenotype. This effect may in part be due to imparting a less responsive central mechanism, characterized by reduced expression of butyrate-sensing receptors in the hypothalamus and possibly other cardioregulatory brain regions in the adult SHR. Future studies should investigate long term role of butyrate in central control of BP in conscious rats.

4 | MATERIALS AND METHODS

4.1 | Animals

Male rats (SHR, WKY) aged 4 and 14-weeks old were purchased from Charles River. All experimental procedures were completed in accordance with the approved protocol #201708217 by the University of Florida Institute for Animal Care and Use Committee, and complied with the standards stated in the National Institutes of Health's Guide for the Care and Use of Laboratory Animals. Rats were housed in a temperature-controlled room (22–23°C) on a 12:12 hour light-dark cycle, in specific pathogen-free cages, and had access to standard rat chow and water ad libitum.

4.2 | SCFA extraction and high performance liquid chromatography

Fecal pellets and cecal contents were collected and subjected to SCFA extraction, as previously described⁵⁵ with some modifications. Briefly, 400 μ L of HCl was added to fecal homogenates to preserve the volatile SCFAs, and vortexed vigorously to evenly suspend the fecal mass. 5 mL of methylene chloride was used to extract the SCFAs with gentle rotation at room temperature for 20 minute. The organic phase was kept after centrifugation at 1500 g for 5 minute. 500 μ L of 1 N NaOH was added to the organic phase, followed by an additional 20 minute. rotation at room temperature. After centrifugation, the top aqueous phase was collected and mixed with 100 μ L of HCl before

being filtered for HPLC. A standard curve was generated with each of the SCFAs investigated: acetate, butyrate, and propionate. Less than 3% of relative standard deviation was achieved by sequential injections of 10 mmol/L standard mixture of all three SCFAs. The peak correlated to each SCFA was identified based on elution time of single injection of each SCFA.

The chromatographic separation was performed at room temperature using Perkin Elmer Series 200 HPLC System (Perkin Elmer Instruments, Norwalk, CT), equipped with an autosampler, quaternary pump, and 200 series UV/VIS detector. The analytical column used was Hypersil Gold aQ 150 \times 4.6 mm 3 μ m (Thermo Fisher Scientific, Waltham, MA). A 50 μ L of extracted samples were injected in a combination of two solutions: 90% of mobile phase A 0.02 mol/L phosphate buffer pH 2.2 and 10% of mobile phase B acetonitrile. Flow rate was set as 0.8 mL/min for 25 minute. Wavelength used for detection was 210 nm.

4.3 | SCFA extraction from serum and liquid chromatography–mass spectrometry

SCFAs were extracted from blood serum as previously described.⁵⁶ Briefly, 100 μ L of blood sera were mixed with 200 μ L of methanol, followed by vigorous vortex. The mixture was centrifuged at 4°C for 10 minute at the speed of 48 000 g. Supernatant was kept for further LC-MS analysis.

The chromatographic separation was achieved using a Thermo Fisher TSQ quantum ultra-mass spectrometer coupled with an Agilent 1100 series Liquid Chromatography system with Xcaliber and LC Quan computing software. A volume of 60 μ L was injected. The butyrate peak was identified based on the elution time determined by single injection of butyrate.

The analytical column was a Thermo Fisher ODS hypersil 250 mm \times 4.6 mm, 5 μ m/L mounted on a column oven set to 35°C. The following gradient was applied. From $t = 0$ to 2 minute 100% solvent A (an aqueous solution of 3 mmol/L hydrochloric acid) was pumped at 0.5 mL/min. From $t = 2$ to 10 minute a linear gradient to 55% solvent B (ethanol/water (95/5: v/v) containing 0.75 mmol/L hydrochloric acid) was applied and pumped at 0.4 mL/min. From $t = 10$ to 12 minute, the gradient was increased to 100% B and maintained at 100% B for 3 minutes. From $t = 15$ to $t = 21$ minute, a return to 100% solvent A was applied at 0.4 mL/min. An additional 4 minute equilibration period with 100% solvent A was used before the next injection. Before entering the MS system, the column effluent was mixed (post column) with 0.15 mol/L ammonia in ethanol, delivered from an additional stand-alone Jasco Model PU 980 (Jasco, Oklahoma City, OK) at 0.5 mL/min which supported negative ionization of the

Butyric acid. The TSQ Quantum ultra was equipped with an orthogonal electro spray (ESI) probe. The MS was operated in negative mode. Measurements were performed in Select Ion Monitoring (SIM) set to $m/z = 87$ with a scan width (m/z) of 1.0. The chrome filter was applied and set to 20 (seconds). Maximum sensitivity was achieved at the following settings: Ion scan time 0.75 seconds, 2 microscans with the capillary temperature set at 140°C. The TSQ system was flushed post sequence from a syringe pump with a 50:50 mixture of Methanol and water to avoid blocking of the heated capillary by ammonium chloride.

4.4 | Ex vivo measurement of butyrate transport in proximal colon

Proximal colon tissues were freshly excised from adult WKY and SHR and mounted in Ussing chambers (Physiologic Instruments, San Diego, CA, USA).⁵⁷ The tissues were bathed in Krebs Ringer buffer on both apical and basolateral sides, maintained at 37°C and continuously gassed with 95% air and 5% CO₂. Krebs Ringer buffer consisted of 118.9 mmol/L NaCl; 25 mmol/L NaHCO₃; 2.4 mmol/L K₂HPO₄; 0.6 mmol/L KH₂PO₄; 1.2 mmol/L CaCl₂; 1.2 mmol/L MgCl₂; 5 mmol/L dextrose. The area of tissue exposed to the Krebs buffer was 0.031 cm². Tissues were allowed a minimum of 10-minute stabilization before 40 mmol/L of butyrate was applied to the apical side of the chamber (luminal). After 60 minute incubation, buffer was collected from chambers on the apical and basolateral sides, and subsequently subjected to LC-MS analysis to determine butyrate levels. Short circuit current (Isc) measurements in response to butyrate were performed using methods similar to those previously described.^{58,59} Briefly, transepithelial voltage was maintained at 0 mV and Isc measured. Basal Isc and delta Isc (condition minus baseline) were reported.

4.5 | Real-time PCR

Proximal colon and partial hypothalamic brain region (coordinates were -1.6 to -2.3 mm caudal to the Bregma, ±1 mm to the midline, and -7 to -8 mm from the brain

surface) were harvested from 14 week-old WKY and SHR. Total RNA was isolated using Trizol, and cDNA was synthesized using Trizol and High Capacity cDNA kit (Thermo Fisher Scientific, Waltham, MA). Real-time PCR was performed and data analyzed as described.⁶⁰ Primers used for butyrate transporters and SCFA-sensing receptors are listed in Table 1.

4.6 | Slc5a8 immunostaining and quantification

Proximal colon sections (4 μm) from adult WKY and SHR were incubated with with SLC5A8 antibody (OABF01657; Aviva Systems Biology, San Diego, CA, USA) and fluorescently labeled with AlexaFluor 488 (S11223; ThermoFisher Scientific) using the following standard protocol. Briefly, sections were rinsed in 1× PBS two times for 2 minutes at room temperature, and incubated with permeabilization solution (0.3% Triton X-100) for 10 minutes at room temperature. Following a further PBS wash, sections were incubated with blocking solution for 20 minutes using 5% normal goat serum, followed by incubation with the primary antibody at a 1:500 dilution overnight at 4°C. Following this, secondary antibody was applied at a 1:500 dilution for 1 hour at RT. The sections were then rinsed in PBS and mounted with anti-fade mounting medium NucBlue (P36983; ThermoFisher). Slc5a8⁺ cells were located on the luminal epithelial border as per previous reports.^{61,62} Images were taken with Keyence fluorescence microscope, and Slc5a8⁺ cells were counted manually using IMAGEJ⁶³ and the counts were normalized to the area surface of each section.

4.7 | Histone H3 and acetylated H3 Western Blot

Adult male WKY and SHR (N = 4/group) were decapitated, and hypothalamus and proximal colon were dissected. Each specimen was rapidly frozen in liquid nitrogen and stored at -80°C until homogenization. Tissues were homogenized in ~200 μL RIPA buffer (150 mmol/L sodium chloride, 1% Triton X-100, 1% deoxycholic acid-

TABLE 1 Primers list

Name	Forward primer	Reverse primer
<i>Ffar2</i>	ATCCTCACGGCCTACATCCT	CAGCAGCAACAACAGCAAGT
<i>Ffar3</i>	GCAAGAGAGTGATGGGGCTT	CGGCTTGGAACTTGGAGGAT
<i>Olfir59</i>	CTTCCAAGTCTGAGCGAGCT	TTGATCACAGGAGGCAGCAG
<i>Slc5a8</i>	CTGGGCTTGTTCCTTTGG	CGTTGTGCGTGCTGTTAC
<i>Slc16a1</i>	GGTGTCAATGGAGGTCTTGGG	GGCCAATGGTCGCTTCTTG
<i>Slc16a3</i>	GGGTCATCACTGGCTTGGGT	GGAACACGGGACTGCCTGC

sodium salt, 0.1% sodium dodecyl sulfate, 50 mmol/L Tris-HCl, 2 mmol/L EDTA, pH 7.5) in the presence of protease inhibitor (Pierce™ Protease Inhibitor Tablets, EDTA-free; Pierce Biotechnology, Waltham, MA). Samples were centrifuged at $16\,000 \times g$ for 20 minutes at 4°C. The supernatants were then collected as total cell lysates. The protein concentration was determined using the Pierce BCA Protein Assay (Thermo Fisher Scientific). Proteins were separated on a Mini-PROTEAN® TGX Stain-Free™ Precast Gels (Bio-Rad, Hercules, CA, USA) and transferred onto PVDF membrane (Trans-blot turbo mini PVDF transfer packs; Bio-Rad). The membrane was blocked in fresh blocking buffer (5% nonfat dry milk in TBST, pH 7.6, containing 0.05% Tween 20) for 1 hour at room temperature and rinsed in TBST buffer (0.05% Tween 20 in 10 mmol/L Tris base, 150 mmol/L NaCl, pH 7.6). Subsequently, the membranes were incubated in the presence of different primary antibodies at 1:1000 dilution (Anti-acetyl-Histone-H3-Antibody, 06-599; Anti-Histone-H3-Antibody, 06-755 from Merck Millipore, Billerica, MA) at 4°C overnight. After washing, membranes were incubated with secondary antibodies (Anti-Rabbit IgG, HRP linked: 1:2000 and Anti-Biotin, HRP-linked at 1:2000 dilution from Cell Signaling, Danvers, MA) at room temperature for 1 hour. The membranes were incubated with Clarity Western ECL substrate (Bio-Rad) and the proteins were visualized using the MP ChemiDoc (Bio-Rad). All images were analyzed by Image Lab software. Target proteins were first normalized to total protein transferred to the blot as per established protocols (bulletin 6427; BioRad) using stain-free technology.

4.8 | ICV injections and blood pressure recordings in anesthetized rats

Adult WKY and SHR rats ($N = 6/5$) were anesthetized with 3% isoflurane and kept under 1.5% anesthesia throughout the experiment. Rats were placed in a stereotaxic frame with their head secured firmly in place by ear bars. ICV injections were performed using a 10 μ L Hamilton syringe needle containing either aCSF or 1 mmol/L butyrate at established stereotaxic coordinates according to Paxinos and Watson rat brain atlas (1.5 cm lateral, 1.0 cm caudal from bregma, and 4 cm ventral to the dorsal surface). 1 μ L of aCSF or butyrate was injected into the lateral ventricle slowly over 30 seconds. BP was recorded before and after the injection via the left femoral artery catheter and monitored in real time using the Spike2 6.16 software (Cambridge Electronic Design Ltd., Cambridge, UK).

The concentration of butyrate applied ICV was based on our preliminary LC-MS data in the serum (1-2 μ mol/L). As the volume of CSF of a 200-300 g rat is 200-300 μ L,⁶⁴ an injection of 1 μ L of 1 mmol/L butyrate results in a final

butyrate concentration of approx. 3-5 μ mol/L, which is within the physiological range of butyrate levels in circulation.^{65,66}

4.9 | Functional magnetic resonance imaging

Rats were assessed for their neuronal responses to centrally administered butyrate using previously published fMRI methods.⁶⁷ The fMRI technique relies on the blood oxygenation level dependent (BOLD) signal, which is associated with hemodynamic mechanisms linked to neuronal and synaptic activity.⁶⁸ Thus, it was used to measure the evoked hindbrain neuronal activity in response to central butyrate.⁶⁹ Adult male WKY and SHR rats ($N = 3$ per group) were initially anesthetized with 3%-4% Isoflurane (delivered in 70%N₂/30%O₂ at 0.1 L/min) during induction and preparations, and then kept between 1.0%-1.5% throughout imaging (~30 minutes per rat, which includes a 10-minute anatomical scan prior to fMRI scanning). Plastic MRI-compatible ICV catheters (Alzet, Cupertino, CA, USA) were implanted in all rats using the established Paxinos-Watson coordinates (lateral 1.5 mm, caudal 1.0 mm, ventral 4.0 mm from Bregma). Images were collected prior to and immediately after a single butyrate injection (ICV, 1 μ L of 1 mmol/L butyrate in artificial CSF), on a 200 MHz (4.7 T-Tesla) Magnex Scientific MR scanner controlled by Agilent Technologies VnmrJ 3.1 console software (Santa Clara, CA, USA).⁶⁷ The selected dose of butyrate was chosen as described in the previous section, and was shown to reduce BP in both strains of rats.

Spontaneous breathing was monitored and recorded during the MRI acquisition (SA Instruments, Stony Brook, NY). Body temperature was maintained at 37-38°C using a warm water recirculation system (Biopac Systems, Inc., Goleta, CA, USA). A 2-shot spin echo echo planar imaging sequence was acquired using the following parameters: TR/TE = 1000/50 ms, and 420 repetitions for a total acquisition time of 15 minute (an image was acquired every 2 seconds), FOV = 32.5 \times 32.5 mm², 12 slices 1.5 mm thick, and data matrix = 64 \times 64. Anatomical scans for image overlay and reference-to-atlas registration were collected using a fast spin echo sequence, with the following parameters: TR/TE_{eff} = 2000/48 ms, RARE factor = 8, and number of averages = 10, FOV = 32.5 \times 32.5 mm², 12 slices 1.5 mm thick, and data matrix = 256 \times 256.

Scans were skull stripped, registered to an atlas of the rat brain, with motion and drift correction. Each subject was registered to a fully segmented rat brain atlas.⁷⁰ A general linear model was used for the first level analysis with a baseline epoch before drug delivery (5 minutes) and a post-stimulus epoch of 10 minutes. All *t*-tests use a 95% confidence level, two-tailed distribution, and heteroscedastic variance assumptions. Higher level between group

random effects analyses were conducted in FMRIB software library (FSL) FEAT program.⁷¹

4.10 | Statistical analysis

Bar graphs were made using Graphpad Prism 6 (San Diego, CA, USA). Statistical analyses included unpaired *t*-test, one-way ANOVA and two-way ANOVA, as indicated in the figure legends.

ACKNOWLEDGMENTS

The authors thank the Advanced Magnetic Resonance Imaging and Spectroscopy (AMRIS) facility for their continued support (National Science Foundation Cooperative Agreement No. DMR-1157490 and the State of Florida). The authors also thank Drs. Craig F. Ferris and Praveen Kulkarni (Northeastern University, Boston) for their providing the rat brain atlas used in the present work. The authors also thank Katelyn Davis, Dr. David Baekey and Shin-Ping Kuan for their technical supports.

CONFLICT OF INTEREST

No conflict of interest to disclose.

ORCID

Tao Yang  <https://orcid.org/0000-0002-4182-9793>

REFERENCES

- Adnan S, Nelson JW, Ajami NJ, et al. Alterations in the gut microbiota can elicit hypertension in rats. *Physiol Genomics*. 2017;49(2):96-104.
- Li J, Zhao F, Wang Y, et al. Gut microbiota dysbiosis contributes to the development of hypertension. *Microbiome*. 2017;5(1):14.
- Yang T, Santisteban MM, Rodriguez V, et al. Gut dysbiosis is linked to hypertension. *Hypertension*. 2015;65(6):1331-1340.
- Mercado J, Valenzano MC, Jeffers C, et al. Enhancement of tight junctional barrier function by micronutrients: compound-specific effects on permeability and claudin composition. *PLoS ONE*. 2013;8(11):e78775.
- Bordin M, D'Atri F, Guillemot L, Citi S. Histone deacetylase inhibitors up-regulate the expression of tight junction proteins. *Mol Cancer Res*. 2004;2(12):692-701.
- Furusawa Y, Obata Y, Fukuda S, et al. Commensal microbe-derived butyrate induces the differentiation of colonic regulatory T cells. *Nature*. 2013;504(7480):446-450.
- Vinolo MA, Rodrigues HG, Nachbar RT, Curi R. Regulation of inflammation by short chain fatty acids. *Nutrients*. 2011;3(10):858-876.
- Yang T, Owen JL, Lightfoot YL, Kladd MP, Mohamadzadeh M. Microbiota impact on the epigenetic regulation of colorectal cancer. *Trends Mol Med*. 2013;19(12):714-725.
- Berni Canani R, Di Costanzo M, Leone L. The epigenetic effects of butyrate: potential therapeutic implications for clinical practice. *Clin Epigenetics*. 2012;4(1):4.
- Gomez-Arango LF, Barrett HL, McIntyre HD, et al. Increased systolic and diastolic blood pressure is associated with altered gut microbiota composition and butyrate production in early pregnancy. *Hypertension*. 2016;68(4):974-981.
- Kim S, Goel R, Kumar A, et al. Imbalance of gut microbiome and intestinal epithelial barrier dysfunction in patients with high blood pressure. *Clin Sci (Lond)*. 2018;132(6):701-718.
- Pluznick JL, Protzko RJ, Gevorgyan H, et al. Olfactory receptor responding to gut microbiota-derived signals plays a role in renin secretion and blood pressure regulation. *Proc Natl Acad Sci USA*. 2013;110(11):4410-4415.
- Pluznick J. A novel SCFA receptor, the microbiota, and blood pressure regulation. *Gut Microbes*. 2014;5(2):202-207.
- Kimura I, Inoue D, Maeda T, et al. Short-chain fatty acids and ketones directly regulate sympathetic nervous system via G protein-coupled receptor 41 (GPR41). *Proc Natl Acad Sci USA*. 2011;108(19):8030-8035.
- Nøhr MK, Egerod KL, Christiansen SH, et al. Expression of the short chain fatty acid receptor GPR41/FFAR3 in autonomic and somatic sensory ganglia. *Neuroscience*. 2015;290:126-137.
- Li G, Su H, Zhou Z, Yao W. Identification of the porcine G protein-coupled receptor 41 and 43 genes and their expression pattern in different tissues and development stages. *PLoS ONE*. 2014;9(5):e97342.
- Tazoe H, Otomo Y, Karaki S, et al. Expression of short-chain fatty acid receptor GPR41 in the human colon. *Biomed Res*. 2009;30(3):149-156.
- Bergersen L, Rafiki A, Ottersen OP. Immunogold cytochemistry identifies specialized membrane domains for monocarboxylate transport in the central nervous system. *Neurochem Res*. 2002;27(1-2):89-96.
- Vijay N, Morris ME. Role of monocarboxylate transporters in drug delivery to the brain. *Curr Pharm Des*. 2014;20(10):1487-1498.
- Sun J, Ling Z, Wang F, et al. *Clostridium butyricum* pretreatment attenuates cerebral ischemia/reperfusion injury in mice via anti-oxidation and anti-apoptosis. *Neurosci Lett*. 2016;613:30-35.
- Stilling RM, van de Wouw M, Clarke G, Stanton C, Dinan TG, Cryan JF. The neuropharmacology of butyrate: The bread and butter of the microbiota-gut-brain axis? *Neurochem Int*. 2016;99:110-132.
- Huuskonen J, Suuronen T, Nuutinen T, Kyrölenko S, Salminen A. Regulation of microglial inflammatory response by sodium butyrate and short-chain fatty acids. *Br J Pharmacol*. 2004;141(5):874-880.
- Braniste V, Al-Asmakh M, Kowal C, et al. The gut microbiota influences blood-brain barrier permeability in mice. *Sci Transl Med*. 2014;6(263):263ra158.
- Reigstad CS, Salmonson CE, Rainey JF, et al. Gut microbes promote colonic serotonin production through an effect of short-chain fatty acids on enterochromaffin cells. *FASEB J*. 2015;29(4):1395-1403.
- Yano JM, Yu K, Donaldson GP, et al. Indigenous bacteria from the gut microbiota regulate host serotonin biosynthesis. *Cell*. 2015;161(2):264-276.

26. Watts SW, Morrison SF, Davis RP, Barman SM. Serotonin and blood pressure regulation. *Pharmacol Rev.* 2012;64(2):359-388.
27. Zubcevic J, Jun JY, Kim S, et al. Altered inflammatory response is associated with an impaired autonomic input to the bone marrow in the spontaneously hypertensive rat. *Hypertension.* 2014;63(3):542-550.
28. Li SG, Lawler JE, Randall DC, Brown DR. Sympathetic nervous activity and arterial pressure responses during rest and acute behavioral stress in SHR versus WKY rats. *J Auton Nerv Syst.* 1997;62(3):147-154.
29. Judy WV, Watanabe AM, Henry DP, Besch HR, Murphy WR, Hockel GM. Sympathetic nerve activity: role in regulation of blood pressure in the spontaneously hypertensive rat. *Circ Res.* 1976;38(6 Suppl 2):21-29.
30. Cates MJ, Dickinson CJ, Hart EC, Paton JF. Neurogenic hypertension and elevated vertebralbasilar arterial resistance: is there a causative link? *Curr Hypertens Rep.* 2012;14(3):261-269.
31. Santisteban MM, Ahmari N, Carvajal JM, et al. Involvement of bone marrow cells and neuroinflammation in hypertension. *Circ Res.* 2015;117(2):178-191.
32. Yang X, Duan B, Zhou X. Long non-coding RNA FOXD2-AS1 functions as a tumor promoter in colorectal cancer by regulating EMT and Notch signaling pathway. *Eur Rev Med Pharmacol Sci.* 2017;21(16):3586-3591.
33. Velázquez OC, Lederer HM, Rombeau JL. Butyrate and the colonocyte. Production, absorption, metabolism, and therapeutic implications. *Adv Exp Med Biol.* 1997;427:123-134.
34. Cummings JH, Pomare EW, Branch WJ, Naylor CP, Macfarlane GT. Short chain fatty acids in human large intestine, portal, hepatic and venous blood. *Gut.* 1987;28(10):1221-1227.
35. Gotoh Y, Kamada N, Momose D. The advantages of the Ussing chamber in drug absorption studies. *J Biomol Screen.* 2005;10(5):517-523.
36. Mascolo N, Rajendran VM, Binder HJ. Mechanism of short-chain fatty acid uptake by apical membrane vesicles of rat distal colon. *Gastroenterology.* 1991;101(2):331-338.
37. Hu J, Lin S, Zheng B, Cheung P. Short-chain fatty acids in control of energy metabolism. *Crit Rev Food Sci Nutr.* 2018;58(8):1243-1249.
38. Bourassa MW, Alim I, Bultman SJ, Ratan RR. Butyrate, neuroepigenetics and the gut microbiome: can a high fiber diet improve brain health? *Neurosci Lett.* 2016;625:56-63.
39. Bienenstock J, Kunze W, Forsythe P. Microbiota and the gut-brain axis. *Nutr Rev.* 2015;73(Suppl 1):28-31.
40. Yang T, Richards EM, Pepine CJ, Raizada MK. The gut microbiota and the brain-gut-kidney axis in hypertension and chronic kidney disease. *Nat Rev Nephrol.* 2018;14(7):442-456.
41. Yang T, Zubcevic J. Gut-brain axis in regulation of blood pressure. *Front Physiol.* 2017;8:845.
42. Mangiola F, Ianiro G, Franceschi F, Fagioli S, Gasbarrini G, Gasbarrini A. Gut microbiota in autism and mood disorders. *World J Gastroenterol.* 2016;22(1):361-368.
43. Casella G, Pozzi R, Cigognetti M, et al. Mood disorders and non-celiac gluten sensitivity. *Minerva Gastroenterol Dietol.* 2017;63(1):32-37.
44. Bergman EN, Wolff JE. Metabolism of volatile fatty acids by liver and portal-drained viscera in sheep. *Am J Physiol.* 1971;221(2):586-592.
45. Bergman EN. Energy contributions of volatile fatty acids from the gastrointestinal tract in various species. *Physiol Rev.* 1990;70(2):567-590.
46. Santisteban MM, Qi Y, Zubcevic J, et al. Hypertension-linked pathophysiological alterations in the gut. *Circ Res.* 2017;120(2):312-323.
47. Henagan TM, Stefanska B, Fang Z, et al. Sodium butyrate epigenetically modulates high-fat diet-induced skeletal muscle mitochondrial adaptation, obesity and insulin resistance through nucleosome positioning. *Br J Pharmacol.* 2015;172(11):2782-2798.
48. Brock JA, Van Helden DF, Dosen P, Rush RA. Prevention of high blood pressure by reducing sympathetic innervation in the spontaneously hypertensive rat. *J Auton Nerv Syst.* 1996;61(2):97-102.
49. Cuff MA, Lambert DW, Shirazi-Beechey SP. Substrate-induced regulation of the human colonic monocarboxylate transporter, MCT1. *J Physiol.* 2002;539(Pt 2):361-371.
50. Borthakur A, Saksena S, Gill RK, Alrefai WA, Ramaswamy K, Dudeja PK. Regulation of monocarboxylate transporter 1 (MCT1) promoter by butyrate in human intestinal epithelial cells: involvement of NF-kappaB pathway. *J Cell Biochem.* 2008;103(5):1452-1463.
51. Febo M, Akbarian S, Schroeder FA, Ferris CF. Cocaine-induced metabolic activation in cortico-limbic circuitry is increased after exposure to the histone deacetylase inhibitor, sodium butyrate. *Neurosci Lett.* 2009;465(3):267-271.
52. Gagliano H, Delgado-Morales R, Sanz-Garcia A, Armario A. High doses of the histone deacetylase inhibitor sodium butyrate trigger a stress-like response. *Neuropharmacology.* 2014;79:75-82.
53. Valvassori SS, Varela RB, Arent CO, et al. Sodium butyrate functions as an antidepressant and improves cognition with enhanced neurotrophic expression in models of maternal deprivation and chronic mild stress. *Curr Neurovasc Res.* 2014;11(4):359-366.
54. Han A, Sung YB, Chung SY, Kwon MS. Possible additional antidepressant-like mechanism of sodium butyrate: targeting the hippocampus. *Neuropharmacology.* 2014;81:292-302.
55. De Baere S, Eeckhaut V, Steppe M, et al. Development of a HPLC-UV method for the quantitative determination of four short-chain fatty acids and lactic acid produced by intestinal bacteria during in vitro fermentation. *J Pharm Biomed Anal.* 2013;80:107-115.
56. van Eijk HM, Bloemen JG, Dejong CH. Application of liquid chromatography-mass spectrometry to measure short chain fatty acids in blood. *J Chromatogr B Analyt Technol Biomed Life Sci.* 2009;877(8-9):719-724.
57. Cheng SX, Lightfoot YL, Yang T, et al. Epithelial CaSR deficiency alters intestinal integrity and promotes proinflammatory immune responses. *FEBS Lett.* 2014;588(22):4158-4166.
58. Ostedgaard LS, Meyerholz DK, Chen JH, et al. The ΔF508 mutation causes CFTR misprocessing and cystic fibrosis-like disease in pigs. *Sci Transl Med.* 2011;3(74):74ra24.
59. Chen JH, Stoltz DA, Karp PH, et al. Loss of anion transport without increased sodium absorption characterizes newborn porcine cystic fibrosis airway epithelia. *Cell.* 2010;143(6):911-923.
60. Yang T, Ahmari N, Schmidt JT, et al. Shifts in the gut microbiota composition due to depleted bone marrow beta adrenergic

- signaling are associated with suppressed inflammatory transcriptional networks in the mouse colon. *Front Physiol.* 2017;8:220.
61. Cresci GA, Thangaraju M, Mellinger JD, Liu K, Ganapathy V. Colonic gene expression in conventional and germ-free mice with a focus on the butyrate receptor GPR109A and the butyrate transporter SLC5A8. *J Gastrointest Surg.* 2010;14(3):449-461.
 62. Takebe K, Nio J, Morimatsu M, et al. Histochemical demonstration of a Na(+)-coupled transporter for short-chain fatty acids (sle5a8) in the intestine and kidney of the mouse. *Biomed Res.* 2005;26(5):213-221.
 63. Schneider CA, Rasband WS, Eliceiri KW. NIH Image to ImageJ: 25 years of image analysis. *Nat Methods.* 2012;9(7):671-675.
 64. Bass NH, Lundborg P. Postnatal development of bulk flow in the cerebrospinal fluid system of the albino rat: clearance of carboxyl-(14 C) inulin after intrathecal infusion. *Brain Res.* 1973;52:323-332.
 65. Wolever TM, Chiasson JL. Acarbose raises serum butyrate in human subjects with impaired glucose tolerance. *Br J Nutr.* 2000;84(1):57-61.
 66. Priebe MG, Wang H, Weening D, Schepers M, Preston T, Vonk RJ. Factors related to colonic fermentation of nondigestible carbohydrates of a previous evening meal increase tissue glucose uptake and moderate glucose-associated inflammation. *Am J Clin Nutr.* 2010;91(1):90-97.
 67. Bruijnzeel AW, Alexander JC, Perez PD, et al. Acute nicotine administration increases BOLD fMRI signal in brain regions involved in reward signaling and compulsive drug intake in rats. *Int J Neuropsychopharmacol.* 2014;18(2):pyu011
 68. Logothetis NK, Pauls J, Augath M, Trinath T, Oeltermann A. Neurophysiological investigation of the basis of the fMRI signal. *Nature.* 2001;412(6843):150-157.
 69. Uğurbil K. Development of functional imaging in the human brain (fMRI); the University of Minnesota experience. *NeuroImage.* 2012;62(2):613-619.
 70. Ferris CF, Yee JR, Kenkel WM, et al. Distinct BOLD activation profiles following central and peripheral oxytocin administration in awake rats. *Front Behav Neurosci.* 2015;9:245.
 71. Jenkinson M, Beckmann CF, Behrens TE, Woolrich MW, Smith SM. Fsl. *NeuroImage.* 2012;62(2):782-790.

SUPPORTING INFORMATION

Additional supporting information may be found online in the Supporting Information section at the end of the article.

How to cite this article: Yang T, Magee KL, Colon-Perez LM, et al. Impaired butyrate absorption in the proximal colon, low serum butyrate and diminished central effects of butyrate on blood pressure in spontaneously hypertensive rats. *Acta Physiol.* 2019;226:e13256. <https://doi.org/10.1111/apha.13256>